

SYNTHESIS AND STRUCTURAL PROPERTIES OF Al_2O_3 - ZrO_2 NANO COMPOSITE PREPARED VIA SOLUTION COMBUSTION SYNTHESIS

RAJU M. BELEKAR, P. S. SAWADH & R. K. MAHADULE

Bapurao Deshmukh College of Engineering, Wardha, Maharashtra, India

ABSTRACT

In this research, an alumina–zirconia composite containing 20 wt % zirconia was prepared by solution combustion synthesis (SCS) method using aluminum nitrate and zirconium nitrate as precursors whereas urea as fuel. The observed X-ray diffraction pattern within temperature range of 600 to 1200°C revealed that with the increase in temperature t-ZrO₂ phase shifted to m-ZrO₂. Moreover the morphological characteristic using FTIR, in corroboration with XRD, confirms the crystallization of corundum (α - Al₂O₃) as one of the alumina phase and monoclinic phase of zirconia at 1200°C. Micro structural characterization by SEM depicted that the particles tend to be more agglomerated with increasing temperature. Comparatively high average pore size of 4nm and surface area of 92m²/g were calculated using BET analyzer.

KEYWORDS: Al₂O₃-ZrO₂, SCS, BET, FT-IR, Surface Area

INTRODUCTION

BACKGROUND

Alumina is one of the most widely used engineering ceramic materials due to its high elastic modulus, high wear resistance and chemical corrosion resistance, high-temperature stability and the retention of strength at high temperatures. However, the drawback of common alumina is its poor mechanical properties, such as flexural strength (about 380 MPa) and fracture toughness (about 3.5 Mpam^{1/2}) [1]. Recently, a bending strength up to 654 MPa and a fracture toughness up to 5.7 Mpam^{1/2} have been obtained for alumina ceramics by using low-temperature-sinter able high purity alumina powder [2]. This alumina will be more widely used for engineering applications if its mechanical properties can be further improved. Zirconia (ZrO₂) has numerous unique properties such as good mechanical strength due to its high toughness, excellent resistance against crack propagation, good thermal resistance, relatively high thermal expansion coefficient, and low thermal conductivity at high temperature [3], which have proven to be superior to other ceramics.

Based on these properties, ZrO₂ nano powders not only have many industrial applications as ceramic bodies, but also can be dispersed as reinforcement in various composite matrixes in order to improve their mechanical properties such as hardness and wear resistance. Studies on the dispersion of ZrO₂ nano powders, which are well known to be present at a low specific surface area, in various matrixes have been reported in literatures [4-8].

In some cases, wear resistance and also properties of sol–gel-derived coatings were improved by dispersing ZrO₂ nano powders in the hybrid matrixes [4]. It is well known that the magnitude of improvement of the mechanical properties depends strongly on the composition, size, and specific surface area of the nano powders. Therefore, the combination of a hard nano structured material like Al₂O₃ with a high toughness ZrO₂ matrix looks as a promising way to produce an excellent composite reinforcement and improve the mechanical properties of the matrix such as hardness,

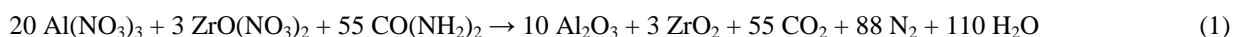
wear resistance, and scratch resistance. Recently great interest in the synthesis of nano-crystalline metal oxides can be seen due to enhanced sinterability, mechanical [9, 10], electrical [11, 12], and chemical properties [13].

Various methods such as milling [14], co-precipitation [15], sol-gel [16] and solution combustion [17-19] have been used to produce oxides nano-powder. Among the available chemical processes, self sustaining solution combustion synthesis is convenient in process, simple in experimental device and time saving. Solution combustion synthesis process involves an aqueous mixture containing suitable metal salts which are the precursors of the final desired oxide and a proper sacrificial organic fuel which acts as reagent reducer.

Generally, hydrate nitrates are preferred to other salts because of their good solubility in water which allows them to obtain a highly homogeneous solution. Urea is the most convenient fuel that can be used in the combustion processes [20] because of its relatively low price, availability, commercially grade and safety.

METHODS

The precursors involved in the present synthesis are aluminum nitrate nonahydrate ($\text{Al}(\text{NO}_3)_3 \cdot 9\text{H}_2\text{O}$), urea $\text{CO}(\text{NH}_2)_2$ and Zirconium nitrate $\text{Zr}(\text{NO}_3)_4 \cdot 5\text{H}_2\text{O}$ all were analytical grade from Merck. The reactions between urea and aluminum nitrate and zirconium nitrate are as relations (1):



The stoichiometric amount of aluminium nitrate, zirconium nitrate and urea were dissolved in 50 ml de-ionized water till clear solution is formed. The solution was then kept on hot plate in order to evaporate more than half of water content. This solution moved to microwave with power of 900 W. After some minutes, first a gel-like structure was obtained and then swelled, followed by the evolution of a large volume of gases. In other word self propagating solution combustion occurred. This reaction product was treated at temperature of 600°C , 1000°C , 1200°C .

CHARACTERIZATIONS

The crystallinity and phase identification of the powders were performed by a Philips Xpert X-ray diffractometer using $\text{Cu K}\alpha$ as the radiation source and Ni as the filter in the 2θ range from 5° - 70° with angular step of $0.02^\circ/\text{min}$. The crystallite size distribution was calculated from the line-broadening method. Using well-known Debye Scherrer equation as follows-

$$D = \frac{0.9\lambda}{B \cos\theta} \quad (2)$$

Where D is crystallite size in nm, λ the wavelength of the radiation, B is the FWHMs observed for the sample, θ is the Bragg's angle. The Fourier Transform Infrared spectroscopy (FT-IR, Vector 22, Bruker) was used to identify the vibrational features of samples. The microstructure of composite membranes supported by hollow fiber microfiltration support and pore size distribution of unsupported membranes were analyzed by scanning electron microscopy (SEM, JSM-6300, JEOL).

The nitrogen adsorption/ desorption isotherms were measured through BET (Brunauer, Emmett and Teller) method [19] ('Micromeritics' equipment) was employed to estimate the specific surface area. A Gaussian function was used to fit the pore size distribution curve.

RESULTS AND DISCUSSIONS

X-Ray Diffraction Study

The XRD analysis patterns of Al₂O₃-ZrO₂ calcinated at various temperature ranging from 600^o C to 1200^o C as shown in figure 1. The zirconium crystallizes early even at lower temperature. At temperature of 600^o C, t-ZrO₂ and m-ZrO₂ phases appears as main content. As the temperature increases the m-ZrO₂ peak found to be dominating t-ZrO₂ phase. As to pure alumina samples, crystalline γ -Al₂O₃ appears at 400^oC, then the γ -Al₂O₃ transforms to θ form above 900^o C and finally, stable α -phase is observed in samples calcinated at temperature above 1200^oC. The XRD pattern of sample calcined at 600^oC is dispersive, and this show that the sample is amorphous state below 600^oC.

The crystal phase of composite membrane is tetragonal ZrO₂ and no diffraction peak of α -Al₂O₃ is observed when the calcining temperature increases from 600^oC to 1000^oC. Moreover the intensity of diffraction peak increases gradually and the breadth of diffraction peak narrows gradually in this temperature region. These indicate that crystal structure becomes integrity and grains grow gradually. At 1200^oC, near the main peak of tetragonal phase zirconia there is a weak peak of monoclinic phase zirconia, and the α -Al₂O₃ appears at same time.

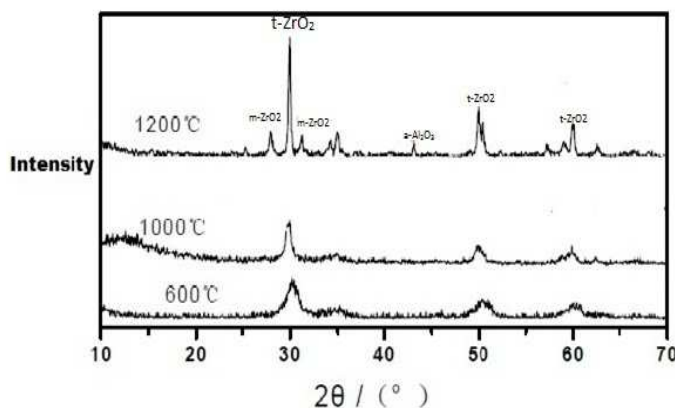


Figure 1: XRD Pattern of Al₂O₃-ZrO₂ (20% wt. ZrO₂)

SEM Analysis

Figure 2 shows the micro structural development of the SCS synthesized Al₂O₃-ZrO₂ composite at various calcinations temperature. The principal merit of the microstructure observed in the alumina-zirconia composites is the adequate relative grain size ratio and phase distribution between the both phases, allowing zirconia particles to be present mostly at grain boundaries without agglomerates. The smaller ZrO₂ particles seem to be entrapped within the alumina grains and the larger ZrO₂ particles seem to remain at the grain boundaries. Stough and Hellmann [21] investigated the solid solubility of zirconia in α -Al₂O₃ and observed that a zirconia solubility of 0.004-0.027 wt% and that tetragonal zirconia (~10 nm) precipitated from supersaturated α -Al₂O₃ and became entrapped within the alumina matrix.

Pugar and Morgan [22] also reported that the development of fine-grained ZrO₂ within the α Al₂O₃ is associated with the $\theta \rightarrow \alpha$ -Al₂O₃ phase transformation. It has been reported that the phase transformation θ to α -Al₂O₃ follows the nucleation and growth process [23]. During the grain growth, a considerable amount of fine pores are redistributed throughout the alumina matrix. Simultaneously, ZrO₂ particles are trapped within the α -Al₂O₃ grains grown from the fine-grained matrix.

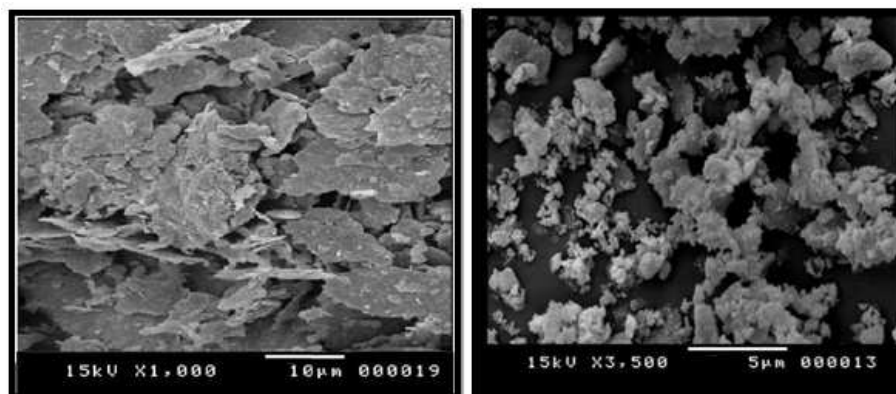


Figure 2: SEM Images of Al₂O₃-ZrO₂ Nano Composite

Fourier Transform –Infrared Spectroscopy

The FTIR results of the samples calcinated at temperature of 1200⁰C is shown in above figure 3. As the calcination temperature increases the absorption peaks becomes flat which is due to evaporation of some organic liquids and water. The major absorption peak is obtained at 2340 cm⁻¹ which corresponds to O=C=O bond vibration. The peak obtained at 1515 cm⁻¹ and 1485 cm⁻¹ attributed to vibration of Zr-OH group bending bands. The peaks seems to be broaden at 3450 cm⁻¹ which is due to vibration of OH- stretching bond. Also, the peaks between 800 and 612 cm⁻¹ correspond to the Al-O vibration [24], whereas the absorption peaks below 670 cm⁻¹ indicate Zr-O bond vibrations [25]. The individual peaks corresponding to Al-O bond and Zr-O bond is obtained only when sample is calcinated at 1200⁰C.

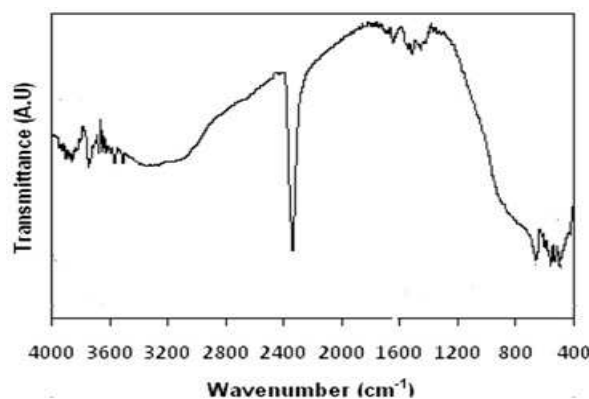


Figure 3: FT-IR Spectroscopy of Al₂O₃-ZrO₂ Calcinated at 1200⁰C

Surface Area Characterization

To obtain detailed information about the pore size, the specific surface area, the meso pore volume and the pore size distribution, a N₂ adsorption and desorption isotherm were performed on the Al₂O₃- ZrO₂ nano powders. The total surface area and pore volume were determined using the BET Eq. (3) and the three point method, respectively.

$$d_{\text{BET}} = \frac{6}{\rho \cdot S} \quad (3)$$

where ρ is the theoretical density of ZrO₂ nano powders, d_{BET} is the particle diameter size and S_{BET} is the specific surface area. The nitrogen adsorption and desorption isotherm curves of the synthesized ZrO₂-Al₂O₃ composite nano powders are shown in Figure 4. These curves show type-IV hysteresis loops that characterize mesoporous adsorbents.

The hysteresis loops in these curves result from wedge-shaped capillaries with a closed edge at the narrower side [26]. The decrease in the difference between the desorption and adsorption curves in the hysteresis loops and their shift to higher relative pressures (P/P_0) with increasing amount of alumina may be ascribed to an increase in the pore size, which consequently leads to decreasing the capillary effect.

Then, the mean pore radii were calculated by the BJH method [27], and the resulting pore size distribution curves are shown in Figure 5. The mean pore diameter of the samples was found to be 4 nm. The specific surface BET areas were obtained from the isotherms for the specimens shown in figure 6. The ZrO₂-Al₂O₃ sample showed specific surface area about 92m²/g.

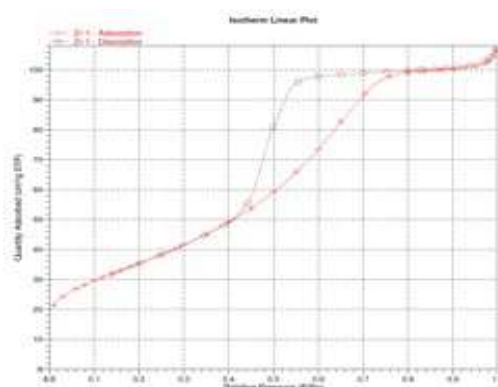


Figure 4: N₂ Adsorption Isotherm of Nano Al₂O₃-ZrO₂ Composite

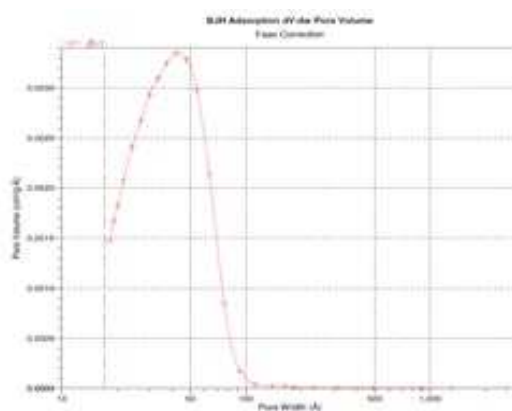


Figure 5: Pore Volume Distribution Curve for Nano Al₂O₃-ZrO₂

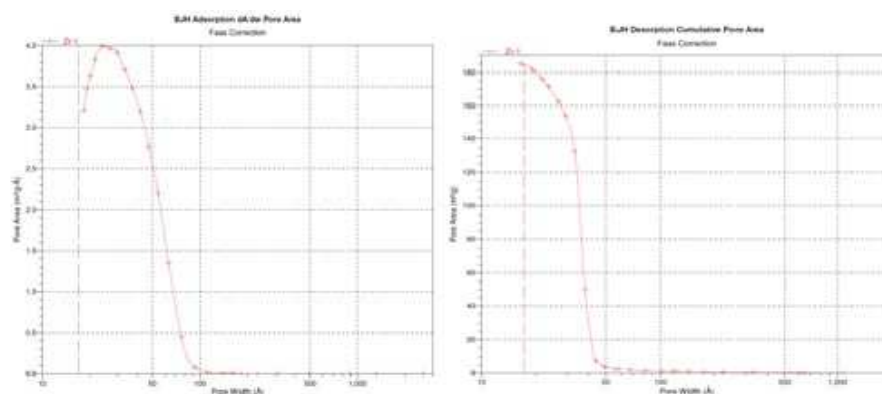


Figure 6: Pore Area Distribution Curve for Nano Al₂O₃-ZrO₂

CONCLUSIONS

In summary, $\text{Al}_2\text{O}_3\text{-ZrO}_2$ nano composite can be prepared via solution combustion synthesis using urea as fuel. XRD pattern and FT-IR studies conformed the formation of α -alumina phase and monoclinic phase of zirconia in $\text{Al}_2\text{O}_3\text{-ZrO}_2$ composite at temperature of 1200°C . The monoclinic phase of zirconia seems to dominate over tetragonal ZrO_2 at higher temperature and converted into monoclinic phase. SEM analysis revealed that the ZrO_2 particle trapped in to alumina matrix. The nitrogen absorption isotherm showed type-IV hysteresis which is a result of presence of wedge shaped capillaries. The average pore size and specific surface area was found to be respectively 4nm and $92\text{ m}^2/\text{g}$.

REFERENCES

1. Munro RG. (1997); *Evaluated material properties of sintered α -alumina*; J Am Ceram Soc; 80:1919.
2. Rao PG, Iwasa M, Kondoh I. (2000) *Properties of low-temperature-sintered high purity alpha-alumina ceramics*; J Mater Sci Lett; 19: 543.
3. Shackelford JF, Doremus RH; (2008). *Ceramic and glass materials: structure, properties and Processin*; Springer, New York.
4. Zheludkevich ML, Salvado IM, Ferreira MGS; (2005); *Sol-gel coatings for corrosion protection of metals*. J Mater Chem; 15:5099–5111.
5. Wang H, XuP ZW, Shen L, Du Q, (2005); *Transparent poly (methyl methacrylate)/silica/zirconia nanocomposites with excellent thermal stabilities*. Polym Degrad Stab; 87:319–328.
6. Yang G, Li J, Wang G, Yashima M, Min S (2005); *Influences of ZrO_2 nanoparticles on the microstructure and mechanical behavior of Ce-TZP/ Al_2O_3 nanocomposites*. J Mater Sci 40: 6087–6090.
7. Adolfsson E, Shen Z (2006), *Densification of zirconia-hydroxyapatite ceramics without phase changes*; Key Eng Mater 309:1141–1144.
8. Mobasherpour I, Hashjin MS, Toosi SSR, Kamachali RD, (2009) *Effect of the addition $\text{ZrO}_2\text{-Al}_2\text{O}_3$ on nanocrystalline hydroxyapatite bending strength and fracture toughness*. Ceram Int, 35, 1569– 1574.
9. X.Y. Teng, H.L. Liu, C.Z. Huang; (2007) *Effect of Al_2O_3 particle size on the mechanical properties of alumina-based ceramics*, Materials Science and Engineering 452-453.
10. S. Jiansirisomboon, A. Watcharapasorn, (2008), *Effects of alumina nano-particulates addition on mechanical and Electrical properties of barium titanate ceramics*, J. Current Applied Physics; 8 48-52.
11. S. Yong, M. Jong, W. Dong, (2008) *Microstructure and electrical conductivity of NiO-YSZ nano- powder synthesized by aerosol flame deposition*, J. Ceramics International; 34 873-876.
12. A. Dima, D. Corteb, F. Williamsa, (2008) *Silicon nano-particles in SiO_2 sol-gel film for nano-crystal memory device applications*, J. Microelectronics 39 768-770.
13. S.W. Tang, P. Zou, H.G. Xiong, (2008); *Effect of nano- SiO_2 on the performance of starch/polyvinyl alcohol blend films*, Carbohydrate Polymers 72 521-526.

14. L. Har, (1990); Alumina chemical, J. Am. Ceram. Soc. 6; 329-334.
15. G. Gimena, H. Xavier (2004), *Nanopowder production a comparison of several methods*, University of Illinois Chicago, NSF-REU Summer.
16. P. Rao, M. Iwasa, T. Tanaka(2003), *Preparation and mechanical properties of Al₂O₃-15wt. %ZrO₂ composites*, J. Scripta Materials 48; 437-441.
17. T.Y. Peng, X. Liu, K. Dai, J.R. Xiao, H.B. Song, (2006) *Effect of acidity on the glycine-nitrate combustion synthesis of nanocrystalline alumina powder*, Materials Research Bulletin 41; 1638-1645.
18. J. Toniolo, M. Lima, A. Takimi, C. Bergmann, *Synthesis of alumina powders by the glycine-nitrate combustion process*, J. Materials Research Bulletin 40 (2005) 561-571.
19. L. Pathak, T. Singh, S. Das, A. Verma, P. Ramachandrarao, (2002) *Effect of pH on the combustion synthesis of nano-crystalline alumina powder*, J. Materials Letters 57; 380-385.
20. K. Tahmasebi, M. Paydar, (2008) *The effect of starch addition on solution combustion synthesis of Al₂O₃-ZrO₂ nanocomposite powder using urea as fuel*, J. Materials Chemistry and Physics; 109; 156-163.
21. M. A. Stough, J. R. Hellmann Jr., (2002) "Solid Solubility and Precipitation in a Single-Crystal Alumina-Zirconia System," J. Am. Ceram. Soc., 85 [12] 2895-902.
22. E. A. Pugar, P. E. D. Morgan, (1986); J. Am. Ceram. Soc., 69 [6] C120-123.
23. Badkar PA, Bailey JE. (1976), *the mechanism of simultaneous sintering and phase transformation in alumina*. J Mat Sci; 11; 1794-806.
24. Chandradass J, Jun B, Bae DS (2008) *Effect of different fuels on the alumina-zirconia nanopowder synthesized by sol-gel auto combustion method*. J Non-Crystalline Solids 354; 3085-3087.
25. Quan Z W, Wang LS, Lin J (2005), *Synthesis and characterization of spherical ZrO₂:Eu³⁺ phosphors by spray pyrolysis process*. Mater Res Bull 40; 810-820.
26. Jayaseelan DD, Rani DA, Nishikawa T, Awaji H, (2000); *Powder characteristics, sintering behavior and microstructure of sol-gel derived ZTA composites*. J Eur Ceram Soc 20: 267-275.
27. Gregg SJ, Sing KSW, (1982); *Adsorption, surface area and porosity*. Academic; New York.

